African Journal of Agricultural Research Vol. 6(32), pp. 6653-6660, 26 December, 2011
Available online at http://www.academicjournals.org/AJAR
DOI: 10.5897/AJAR11.1112
ISSN 1991-637X ©2011 Academic Journals

Full Length Research Paper

Relations between surface evapotranspiration and water table: A case study base on remote sensing

Aidi Huo[1,3]*, Hua Li[2], Ming Hou[2] and Changlu Qiao[3]

[1]School of Environmental Science and Engineering, Chang'an University, Xi'an Shaanxi 710054, China.
[2]School of Environment and Resource Northwest Sci-Tech University of Agriculture and Forestry, Yangling, Shaanxi, 712100, China.
[3]School of Water Conservancy North China University of Water Resources and Electric Power, Zhengzhou, 450011,China.

Accepted 13 September, 2011

Estimation of land surface evapotranspiration (ET) is one of the most difficult tasks in the field of hydrology and water resources. In this study, ET in the Golmud Region is estimated using remote sensing techniques, which own the characteristics of high efficiency, precision, large-scale and visualization. The Golmud Region has a specific geographic feature and it is an important mineral production base in China. However, the health of ecosystem in this region is just enduring severe water resources stress. Surface energy balance system model being an applicable model with good theoretic basis to estimate land surface ET with less meteorological data requirement, and the improved model is used to estimate land surface ET and analyzes the relationship with the water level in the Golmud Region on the basis of MODIS data. Results show that annual ET is single-peak distributed in month scale with a well seasonal variation. Spatially, Land surface spatial distribution of ET from south to north, from high altitude to low altitude mountain plain, ET following a decrease in the ground water table, so come to that the groundwater depth is the most important controlling factor of ET. The improved model is also suitable for other similar areas.

Key words: Land surface evapotranspiration, remote sensing, MODIS, Golmud Region.

INTRODUCTION

ET plays an important role in the global hydrological cycle, which includes evaporation and transpiration. ET is always the important research subjects on hydrology, soil, agriculture, meteorology; ET also has important applications in water resources in arid areas, regional planning and management of agricultural production (Prince, 1984; Bastiaanssen, 2000). There are many traditional ET computation methods which generally include two steps: First, calculate reference ET (Ray et al., 2002) and second, ET multiplies by crop coefficient which varied for different crops and their growth stages (Ray et al., 2001; Kashyap et al., 2001; Soer, 1980). The traditional computation methods can be classified into three types: temperature methods, radiation methods and combination methods which are based on the original Penman combination equation that consists of two terms: the radiation term and the aerodynamic term (Jacod et al., 2001). Moreover, ET can be measured quite accurately using apparatus such as weighing hypsometers (Liu et al., 2002) and TDR (Time-Domain Reflectometer) (Mastrorilli et al., 1998), but all these ET computation and measurement methods are limited because they only provide point values of ET for a specific location rather than provide ET on a regional scale.

Actually, ET is highly variable in both space and time. Terra and Aqua Satellite images provide an excellent means for determining and mapping the spatial and temporal structure of ET. Remote sensing methods are attractive to estimate ET as they cover large areas and can provide estimates at a very high resolution (Kite and Droogers, 2000). Some researchers developed several Remote Sensing methods to compute ET. Granger (2000) used satellite-derived feedback mechanism to

*Corresponding author. E-mail: huoaidi@163.com.

Figure 1. Location of the Golmud region in China.

compute ET. Choudhury (2000) developed a biophysical model which linked the water, energy and carbon processes by using satellite and ancillary data to quantify ET and biomass production. Bastiaanssen et al. (1998) developed a model named SEBAL (Surface Energy Balance Algorithm for Land) which is comprised of 25 sub models (Kite and Droogers, 2000; Choudhury, 2000; Bastiaanssen et al., 1998).

SEBAL was used by many researchers to study ET (Prince, 1984; Caselles et al., 1998; Chemin and Alexandris, 2001; Timmermans and Maijerink, 1999). It consists of the following: a set of tools for the determination of the land surface physical parameters from spectral reflectance and radiance, such as albedo, emissivity, temperature, vegetation coverage etc. from spectral reflectance and radiance (Su, 2002); an extended model for the determination of the roughness length for heat transfer (Su and Jacob, 2001). In the present set-up, SEBAL requires three sets of information as inputs. The first set consists of land surface albedo, emissivity, temperature, fractional vegetation coverage and leaf area index, and the height of the vegetation. When vegetation information is not explicitly available, the Normalized Difference Vegetation Index (NDVI) is used as a surrogate. These inputs can be derived from remote sensing data in conjunction with other information about the concerned surface. The second set includes air pressure, temperature, humidity, and wind speed at a reference height.

The reference height is the measurement height for point application and the height of the planetary boundary layer (PBL) for regional application. This data set can also be variables estimated with a large scale meteorological model (Gutman and Ignatov, 1998). The third data set includes downward solar radiation, and downward long wave radiation which can either be measured directly, model output or parameterizations. Remote sensing methods used for determination of land surface physical parameters can be found elsewhere (Su, 2002; Su and Jacob, 2001; Gutman and Ignatov, 1998; Su, 2000); the emphasis of the present study is on the new formulation of SEBAL and its validation with four different data sets.

In this study the SEBAL model was used to compute ET of the Golmud region (GR) of China, then spatial and temporal analyze to ET was carry on. The Golmud River is the main fresh water source for the people living in Golmud region, and the total water amount available from the Golmud River is decreasing in recent years. This study is helpful for the proper utilization of water resource of the Golmud River. The method can be extended to temporal and spatial distribution of ET of other similar areas.

MATERIALS AND METHODS

Study area

"Golmud" means a dense river area as a Mongolian word. Geographic Golmud is located in the southern margin of the Qaidam Basin, between 94°35' and 95°05' east longitude, 36°08' and 36°30' north latitude, with an average altitude of 2800 m (Figure 1). Being in the vicinity of the Eurasian continent, the warm

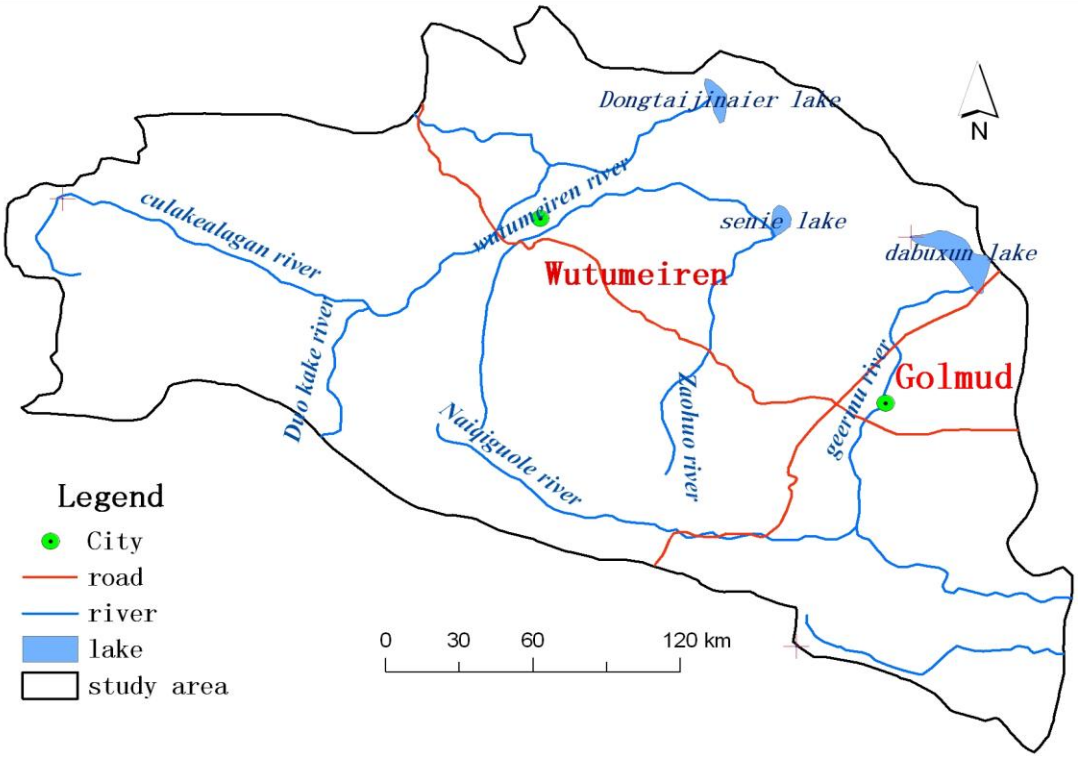

Figure 2. Study area and hydrologic distribution.

air come from southwest is difficult to enter this area due to the barrier layers caused by the Himalayas mountains, the Tanggula mountains and the Kunlun mountains, this situation formed a extreme drought continental climatic characteristics with strong solar radiation, strong evaporation, low air pressure and windy. The average annual rainfall is 40.6mm but the average annual evaporation is 2709.7mm in this region.

The geographical distribution of ET and precipitation are totally discord with each other, reveals in space as low in the north and high in the south. The annual average evaporation of this region is generally between 1200 to 2000 mm and it is significant that the precipitation and evaporation subject to the geographical and altitude in Golmud River basin. With raising in altitude by 100 meters increases precipitation by 12 mm, and reduces evaporation by 70 mm.

Data sets

This study used two data sets: MODIS satellite image dataset and ground measurement dataset.

MODIS image dataset

The MODIS reflectivity data used in this study is the 16 days synthesis data of 500 m spatial resolution in July 2009, which can be used to monitor the Earth's vegetation, its seasonal changes and the inter-annual changes. This dataset has been widely used in eco-environmental change study (Knight et al., 2006). It was downloaded from the web site of earth observing system (EOS) of NASA. Images have preliminary been preprocessed and analyzed, improvement such as radiometric and atmospheric correction have been done. The quality of the available dataset was improved by removal of some noise influential points. The MODIS 1, 2, 3, 4, 5, 6, and 7 reflection band ($\alpha_{1\text{-}7}$) were composted and also be used.

Field surveys dataset

Field investigations and ground measurement were carrying on in Golmud-nanshankou for the ET, vegetation, soil and groundwater data on July 2009. Also field surveys and data collections for the vegetation species, vegetation in some typical areas, the suitable depth of groundwater, the suitable unsaturated zone, water content and salinity have been done. Location of the survey sites are shown as Figure 3.

Regional ET of the two-resistance model

The surface energy balance is commonly written as (Yunhao et al., 2005):

$$LE = R_n - H - G \quad (1)$$

Where R_n is the net radiation, G is the soil heat flux, H is the turbulent sensible heat flux, and LE is the turbulent latent heat flux (L is the latent heat of vaporization and E is the actual ET), their unit is W/m^2.

Non-uniform surface is formed by the vegetation and bare ground. Apparently, the corresponding water heat exchange process of the vegetation and the bare ground are different. Two-impedance model will fully take into account that the canopy microclimates have different effects on soil and vegetation. Thus, the model parameterized respectively for the soil and vegetation.

The energy balance equation in the vegetation coverage areas and bare soil area will be expressed as:

$$LE_v = R_{nv} - H_v - G_v \quad (2)$$

$$LE_g = R_{ng} - H_g - G_g \quad (3)$$

Therefore, the calculation of regional ET becomes the calculation of the $R_{nv}, R_{ng}, H_v, H_g, G_v$ and G_g. Where, LE_v is vegetation canopy latent heat flux, LE_g is the soil surface latent heat flux; R_{nv} and R_{ng} is the net radiation into vegetation canopy and soil surface, respectively; H_v and H_g is the sensible heat flux of vegetation canopy and soil surface, respectively; G_v and G_g is the soil heat flux into the vegetation canopy and soil surface, respectively. The unit of all parameters is W/m^2.

Obtain model parameters

Vegetation canopy and soil surface net radiation (R_{nv}, R_{ns})

Vegetation canopy and soil surface net radiation can be expressed as Equations (4) and (5):

$$R_{nv} = f_v R_n \quad (4)$$

$$R_g = (1 - f_v) R_n \quad (5)$$

Where f_v is the ratio of vegetation covered area in the unit area, there is following formula f_v and NDVI (Gutman and Ignatov, 1998):

$$f_v = \frac{NDVI - NDVI_{\min}}{NDVI_{\max} - NDVI_{\min}} \quad (6)$$

Where $NDVI_{\max}$ and $NDVI_{\min}$ are the maximum and minimum NDVI during the growing season (taken 0.92 and 0.005 in this article).

Vegetation canopy and soil surface heat flux (G_v, G_g)

In the double model, the net heat flux into the vegetation coverage area can be expressed as a function of radiation (Yaoming and Jiemin, 1999):

$$G_v = \frac{T_v}{\alpha}(0.0032\alpha + \alpha^2)(1 - 0.978NDVI^4)/R_n \quad (7)$$

Where T_v is vegetation canopy temperature; α is surface albedo. In the bare land, it is a linear relationship between soil heat flux and net radiation (Renhua et al., 2002):

$$G_g = 0.40 \times R_n \quad (8)$$

Surface net radiation (R_n)

Radiation energy is the main energy ET. The equation to calculate the net radiation is given by (Harfield et al., 1983):

$$R_n = Q(1-\alpha) + \varepsilon_a \sigma T_a^4 - \varepsilon_s \sigma T_s^4 \quad (9)$$

Where Q is sun radiance on the land surface, α is the surface albedo, σ is Stefan-Boltzman constant ($\sigma = 5.6696 \times 10^{-8} Wm^{-2}K^{-4}$), $\varepsilon_a \sigma T_a^4$ is Atmospheric long-wave radiation, ε_α and ε_s is the emissivity of the atmosphere and land surface, T_α is atmosphere temperature, T_s is land surface temperature. Among them, the parameters ε_α can be estimated through following formula (Hartfield et al., 1983):

$$\varepsilon_\alpha = 0.92 \times 10^{-5} T_\alpha^2 \quad (10)$$

Because of soil emissivity (ε_s) is generally between 0.90 to 0.95 (GuoYu et al., 2006) so the average value of 0.925 to be used to calculate the net long wave radiation; According to the relations of surface temperature and temperature,

$$T_a = 0.0473 \times T_s^2 + 2.8111 \times T_s - 18.459$$

Surface albedo parameters (α)

The albedo α is obtained through compositing the MODIS 1,2,3,4,5,6,7 reflection band ($\alpha_{1\text{-}7}$) (Equation 11); Land surface temperature T_s can be acquired from the thermal infrared remote sensing data (Aidi et al., 2008):

$$\alpha = 0.3973\alpha_1 + 0.2382\alpha_2 + 0.3489\alpha_3 - 0.2655\alpha_4 + 0.1604\alpha_5 - 0.0138\alpha_6 + 0.0682\alpha_7 + 0.0036 \quad (11)$$

Where α_i represent the MODIS 1-7 bands narrowband albedo.

Sensible heat flux (H)

Sensible heat flux is heat per unit area of surface transfer by release and absorption. The change of sensible heat flux has the relationship with characteristics of atmospheric boundary layer turbulence (Jie et al., 2005), can be expressed as:

$$H = \rho C_p (T_s - T_a)/r_a \quad (12)$$

Where H is the sensible heat flux; ρ is the density of air (kg/m^3), dry air at standard atmospheric pressure and 20°C, the density ρ =

1.2 Kg/m^3; C_p is the air specific heat (= 1004J/kg / K); T_s is the surface or canopy temperature (K); T_a is the reference height air temperature (K); r_a is the aerodynamic resistance, and aerodynamic impedance is r_{a0} in the neutral stratification.

Aerodynamic resistance (R_α)

In considering the non-neutral stratification conditions, the aerodynamic resistance can be expressed as (Changyao et al., 2001):

$$r_\alpha = r_{\alpha 0} \times \{1 + \phi[\ln(Z-d)/Z_0]\} \quad (13)$$

$$r_{\alpha 0} = [\ln(Z-d)/Z_0]^2 / K^2 U_{(z)} \quad (14)$$

Where $r_{\alpha 0}$ under neutral stratification that the aerodynamic resistance (S.m^{-1}); ϕ is the stability coefficient and can be calculated by the correction factor calculations (Changyao et al., 2001; Ambast et al., 2002). Z is the height of air temperature and humidity measurements (m), takes 2m generally, grass takes 0.2m and shrub takes 0.8m; Z_0 is the surface roughness length (m), $Z_0 = 0.13Z$, bare soil surface roughness takes 0.01m; d is zero plane displacement (m), $d = 0.63Z$; K is the Von Karman constant, takes 0.4; $U_{(z)}$ is the wind speed at reference height Z (m.S^{-1}).

In the case of neutral stratification, when the vegetation height take 0.2 m and $U_{(z)}$ take 2 $m \cdot s^{-1}$, the aerodynamic resistance of vegetation coverage area and the bare soil area can be calculated out according to the above formulas, they are 149.93 $s \cdot m^{-1}$ and 87.73 (Yunhao et al., 2001) respectively. According to the regional characteristics, vegetation height Z (m) values were 0.1, 0.8, 0.8 and 0.1 in four seasons, zero plane displacement d is 0.63 h and roughness Z_0 is 0.13 h.

***Surface temperature* (T_s, T_v, T_g)**

There is the following relationship in Non-uniform land surface temperature, vegetation cover and soil surface temperature (Siu et al., 1997):

$$\varepsilon_s \sigma T_s^4 = f_v \varepsilon_v \sigma T_v^4 + (1-f_v)\varepsilon_g \sigma T_g^4 \quad (15)$$

The temperature of each pixel is actually a weighted sum of vegetation cover and bare soil temperature, that is:

$$T_s = f_v T_v + (1-f_v) T_g \quad (16)$$

Where T_s, T_v and T_g are the average land surface temperature, vegetation canopy temperature and soil surface temperature respectively. ε_v and ε_g are emissivity of vegetation and bare soil, selects 0.93 and 0.97, respectively (Siu et al., 1997), therefore, the unit pixel emissivity can be expressed as

$$\varepsilon_s = f_v \times 0.93 + (1-f_v) \times 0.97 \quad (17)$$

In addition, the average land surface temperature T_s can be retrieved from the MODIS brightness temperature data[1]. Accordingly, the solution of simultaneous Equations (15) and (17) will offer T_g and T_v .

Instantaneous ET and diurnal ET

Diurnal ET data is need in practice but the estimate value of ET is retrieved from remotely sensed satellite image data with different time scale. A widely used approach is weighting method (Yunhao et al., 2005):. It assumptions that the diurnal changes in ET and the solar irradiance are similar under cloudless weather conditions, the relations between this two parameters can be expressed as sine approximation (Yunhao et al., 2005):

$$\frac{E_d}{E_i} = \frac{2N_E}{\pi \cdot \sin(\pi t / N_E)} \quad (19)$$

Where E_d is diurnal ET; E_i is the satellite transit instantaneous ET; N_E is the daylight period from sunrise to sunset; t is the interval between sunrise and time *i*. N_E is calculated by follow equations (Jackson et al., 1983):

$$N_E = 0.945\{c + d\sin^2[\pi(D+10)/365]\} \quad (20)$$

$$c = 12.0 - 5.69\times10^{-2}L - 2.02\times10^{-4}L^2 + 8.25\times10^{-6}L^3 - 3.15\times10^{-7}L^4 \quad (21)$$

$$d = 0.123\times L - 3.10\times10^{-4}L^2 + 8.00\times10^{-7}L^3 + 4.99\times10^{-7}L^4 \quad (22)$$

Where *c* and *d* are latitude dependent constants; *c* is the shortest daylight of the year; *d* is the amount that must be added to *c* in order to obtain the longest daylight of the yea. D is the number of days in the year; L is local latitude (Zhang and Lemeur, 1995). It is easy to calculate diurnal ET and applicable for the use of remote sensing data in this method.

RESULTS AND ANALYSIS

This article mainly discusses the distribution characteristics and relations between regional surface ET and water table base on remote sensing data support. Further analysis was conducted for the purpose of comparing the model calculated ET and the real pan evaporation under monthly scale and diurnal scale respectively. The analysis show that the actual monthly ET is significantly less than the pan evaporation and the monthly ET at maximum

Table 1. Comparison between remote sensing retrieval Diurnal ET value and ground validation ET value.

Measured points	Center longitude	Center latitude	Groundwater depth/m	NDVI	Diurnal ET (mm)	Measured value	Error
TJ1	94°48′04″	36°27′00″	0.21	0.471	8.31	8.11	0.20
TJ2	94°54′33″	36°34′21″	0.23	0.573	8.60	7.98	0.62
TJ3	95°07′23″	36°43′39″	0.80	0.380	9.72	10.12	0.40
TJ4-6	95°02′42″	36°39′28″	2.20	0.378	9.55	9.77	0.22
TJ7	95°09′02″	36°26′21″	1.70	0.406	9.12	8.96	0.16
TJ8-13	94°51′38	36°29′40	0.20	0.571	8.18	7.54	0.64

frequencies is in agreement with other relevant researches, the typical diurnal ET is similar to the relevant researches. Therefore, the simulation result of this model is reasonable.

Validation

Validation works were conducted in July, 2009. As it is shown in Table 1, the exploratory well TJ3 (where the land surface covered a thick salt crust about 25 centimeters, bared salt marsh without any vegetation) has the maximum measurement ET of 10.12 mm as well as the model calculated diurnal ET, 9.72 mm. A significant cause of the great ET is that the groundwater table is only 0.8 m depth there. Exploratory well TJ4-6 (reed and the shrub mixed) has a second greater measurement ET, the model calculated diurnal ET is 9.55 mm, total vegetation coverage there is as low as 25% and the groundwater depth is 2.2 m. Wildcat well TJ7 (shrubbery) has a third diurnal ET value, 9.12 mm, and a third measured ET value. There salt crust cover the surface is about 10 cm, vegetation coverage is 50% and the groundwater depth is 1.7 m. Wildcat well TJ8-13 (shrub forest, carex marsh and beaches dwarf reed) has the minimum value of measured ET, 7.54 mm, as well as the model calculated ET, 8.18 mm. The forest vegetation there is mainly white thorn, haloxylon and reed, total coverage is 70% and the groundwater depth is only 0.2 m because the west Golmud river flows through the eastern, and a riverbed with unknown name occupies the western. The survey results show that vegetation coverage and groundwater depth are two main factors affecting the ET. The lower vegetation coverage and shallower groundwater depth is, the greater ET is. Comparison between remote sensing retrieval and ground validation is shown in Table 1.

Groundwater level and ET

As the amount of precipitation and natural runoff is very small in Golmud region, the consumption of ET mainly comes from the groundwater, and the ET is also the main drainage channel of the groundwater there. So, one can study the groundwater evaporation by study its two main section, soil evaporation and plant transpiration. Comparison analysis on the relationship of ET, water table and vegetation reveals that along with the groundwater table raise gradually, the ET increase accordingly from the southern part to the northern part of Golmud region; salinate fields and Salinity Lake have the maximum ET value. While the groundwater level changes have also caused changes in vegetation distribution.

Groundwater level is an important factor that affecting the ET in arid areas such as Golmud. In arid areas with shallow groundwater depth, groundwater evaporation even plays a key role in the discharge of ground water. The depth of groundwater level influences the evaporation constantly, and it is generally believed that there is a "depth limit" where the groundwater evaporation is close to zero when the depth of underground water is greater than it, without considering the evaporation. In the southern part of Golmud hillside, the rising height of capillary water is very small because of the coarse grain in soil, meanwhile the groundwater depth is greater than other areas, so the groundwater can not up to the ground surface. It caused rare vegetation in this region and very small ET, even close to zero at some part of this region. Because there is a shallow groundwater depth less than 1 m. the ET is large in most salt lake area although there is even no vegetation there.

From everything, it can be concluded that in Golmud and other drought areas like it, the depth of groundwater is the major factor affecting ET.

DISCUSSION

Based on MODIS remote sensing data, the value of ET and spatial distribution is obtained in Golmud region through ET model (Figure 2). The minimum value of instantaneous ET in the study area is 0.02 mm, and the maximum value is 2.66 mm, the minimum of diurnal ET is 0.20 mm, and the maximum is 17.40 mm, the average is 7.68 mm. In space, the evaporation of piedmont Gobi gravel area tends to zero meanwhile with a deep groundwater level; in the plain areas, groundwater is shallow meanwhile with the distribution of the oasis zone,

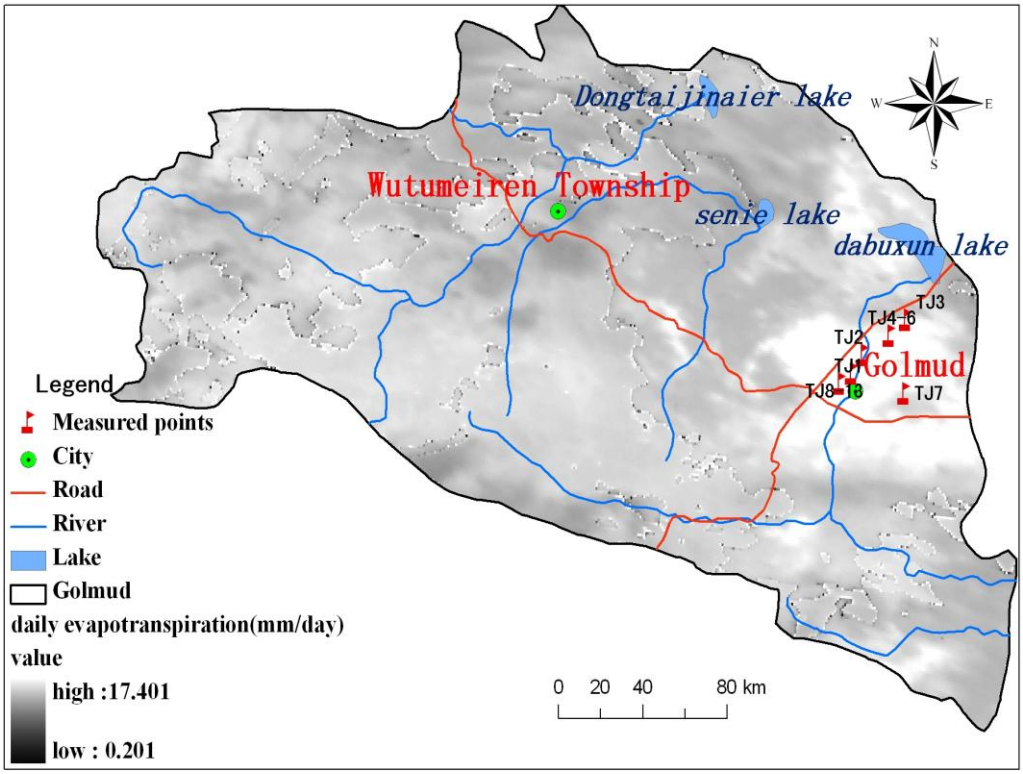

Figure 3. Spatial distribution of Diurnal ET.

the vegetation transpiration and soil evaporation are very strong and the ET is large there; in salt crust lakes, groundwater buried deep and little vegetation there, the ET dominated by soil evaporation. This distribution of vegetation is ideal for the establishment of ET model base on MODIS data. In the study area, the groundwater depth gradually becomes shallow from south to north, as well as the altitude from high to low. At the same time, the ET also increases; it suggests that groundwater depth is an important control factor of ET in this area. Vegetation-covered areas, oasis areas, saline areas with shallow groundwater depth, lush grassland zone, near water bodies and Gobi desert and the bare area, the distribution of various components of Golmud region is significantly different from other regions around. Through the analysis on the distribution of each component, one can clearly find that the distribution of each component shows obvious zonality. It also can be found that vegetation cover on land surface has a great influence on ET, it will make a big different ET with or without vegetation cover underlying surface.

Conclusion

The method for calculating the surface ET in this article has the potential to get regional distribution of ET effectively, improve the understanding of the water consumption of different crop, and support regional water resources assessment. However, there are still some problems such as the model is not mature yet when use it in steep mountain area, a large number of empirical field data used in the model needed to verify and sometimes the results need to be amend manually based on the actual situation, etc., These deficiencies will have to be improved in the future work.

ACKNOWLEDEGEMENTS

This work was sponsored by Project CHD2011JC028 of the Fundamental Research Funds for the Central Universities. The authors also acknowledge the Program for Changjiang Scholars and Innovative Research Team in University of Ministry of Education of China (IRT0811)-PCSIRT and National Natural Science Foundation of China (project number 41072183).

REFERENCES

Price J (1984). Land surface temperature measurements from the split window channels of the NOAA 7 Advanced Very High Resolution Radiometer[J]. J. Geophys. Res., 89(D5): 7231-7237.

Bastiaanssen W (2000) SEBAL-based sensible and latent heat fluxes in the irrigated Gediz Basin, Turkey[J]. J. Hydrol., 229(1-2): 87-100.

Ray S, Dadhwal V, Navalgund R (2002). Performance evaluation of an irrigation command area using remote sensing: A case study of Mahi

command, Gujarat, India[J]. Agric. Water Manage, 56(2): 81-91.
Ray S, Dadhwal V (2001). Estimation of crop evapotranspiration of irrigation command area using remote sensing and GIS[J]. Agricultural Water Manage., 49(3): 239-249.
Kashyap PS, Panda R (2001). Evaluation of evapotranspiration estimation methods and development of crop-coefficients for potato crop in a sub-humid region[J]. Agric. Water Manage., 50(1): 9-25.
Soer G (1980). Estimation of regional evapotranspiration and soil moisture conditions using remotely sensed crop surface temperatures[J]. Remote Sens. Environ., 9(1): 27-45.
Jacobs J, Satti S, Fitzgerald J (2001). Evaluation of reference evapotranspiration methodologies and AFSIRS crop water use simulation model[J]. Publ SJ2001-SP8 Available online at http://www sjrwmd com/programs/outreach/pubs/techpubs/sj2001-sp8 pdf (Verified 20 October, 2003).
Liu C, Zhang X, Zhang Y (2002). Determination of daily evaporation and evapotranspiration of winter wheat and maize by large-scale weighing lysimeter and micro-lysimeter[J]. Agric. For. Meteorol., 111(2): 109-120.
Mastrorilli M, Katerji N, Rana G (1998). Daily actual evapotranspiration measured with TDR technique in Mediterranean conditions[J]. Agric. For. Meteorol., 90(1-2): 81-89.
Kite G, Droogers P (2000). Comparing evapotranspiration estimates from satellites, hydrological models and field data[J]. J. Hydrol., 229(1-2): 3-18.
Choudhury B (2000). Seasonal and interannual variations of total evaporation and their relations with precipitation, net radiation, and net carbon accumulation for the Gediz basin area[J]. J. Hydrol., 229(1-2): 77-86.
Bastiaanssen W, Menenti M, Feddes R (1998). A remote sensing surface energy balance algorithm for land (SEBAL). 1. Formulation[J]. J. Hydrol., 212: 198-212.
Caselles V, Artigao M, Hurtado E (1998). Mapping actual evapotranspiration by combining Landsat TM and NOAA-AVHRR images: application to the Barrax area, Albacete, Spain[J]. Remote Sens. Environ., 63(1): 1-10.
Chemin Y, Alexandridis T, Sensing R (2001). Improving spatial resolution of ET seasonal for irrigated rice in Zhanghe, China.
Timmermans W, Meijerink A (1999), Remotely sensed actual evapotranspiration: implications for groundwater management in Botswana[J]. Int. J. Appl. Earth Observ. Geoinf., 1(3-4): 222-233.
Su Z (2002). The Surface Energy Balance System (SEBS) for estimation of turbulent heat fluxes[J]. Hydrol. Earth Syst. Sci., 6(1): 85-99.
Su Z, Jacobs C (2001). Advanced Earth Observation–Land Surface Climate (Report USP-2).
Gutman G, Ignatov A (1998). The derivation of the green vegetation fraction from NOAA/AVHRR data for use in numerical weather prediction models[J]. Inter. J. Remote Sens., 19(8): 1533-1544.
Su Z (2000). Remote sensing of land use and vegetation for mesoscale hydrological studies[J]. Inter. J. Remote Sens., 21(2): 213-233.
Yunhao C, Xiaobing L, Jing L (2005). Simple Two-component Structure Model for Daily Evapotranspiration[J]. Geomatics Inf. Sci. Wuhan Univ., 30(012): 1075-1079.
Gutman G, Ignatov A (1998). The derivation of the green vegetation fraction from NOAA/AVHRR data for use in numerical weather prediction models[J]. Inter. J. Remote Sens., 19(8): 1533-1543.
Yaoming M, Jiemin W (1999). Estimation of flux densities over the heterogeneous land surface with the aid of satellite remote sensing and field observation[J]. Acta Meteorol. Sin., 57(002): 180-189.
Renhua Z, Xiaomin S, Zhillin Z (2002). To differential thermal inertia-based remote sensing information model of surface evaporation and the whole desert region in Gansu authenticatio[J]. Sci. China: D Ser., 32(012): 1041-1050.
Hatfield J, Reginato R, Idso (1983). Comparison of long-wave radiation calculation methods over the United States[J]. Water Resour. Res., 19(1): 285-288.
GuoYu Q, Shuai W, Xiao W (2006). Three temperature(3t) model-a method to estimate evapotranspiration and evaluate environmental quality[J]. J. Plant Ecol., 30(002): 231-238.
Aidi H, zhili L, xiangwu K (2008). Research in retrieval of land surface temperature in Aeolian desertification areas from MODIS image data[J]. Chinese High Technol. Lett., 18(005): 511-518.
Jie Z, xingguo Y, yaohui L (2005). Estimation of surface energy and day evapotranspiration in a dry2 farming region of Northwest China using satellite data[J]. Chinese J. Geophys., pp. 6-48.
Changyao W, Zheng N, huajun T (2001). Earth observation technology and precision agriculture[J]. beijing: Beijing Science Press, pp. 82-100.
Ambast S, Keshari A, Gosain A (2002). An operational model for estimating regional evapotranspiration through surface energy partitioning (RESEP)[J]. Inter. J. Remote Sens., 23(22): 4917-4930.
Yunhao C, Xiaobing L, Peijun S (2001). Regional Evapotranspiration Estimation over Northwest China Using Remote Sensing[J]. Acta Geogr. Sin., 56(003): 261-268.
Sui H, Tian G, Li F (1997). Two-layer model for monitoring drought using remote sensing[J]. J. Remote Sens., 1(3): 220-224.
Jackson R, Hatfield J, Reginato R (1983). Estimation of daily evapotranspiration from one time-of-day measurements [J]. Agric. Water Manage., 7(1-3): 351-362.
Zhang L, Lemeur R (1995). Evaluation of daily evapotranspiration estimates from instantaneous measurements[J]. Agric. For. Meteorol., 74(1-2): 139-154.